

Paper

Evaluation of Detection Efficiency of Atom Probe Tomography

Masato Morita^{1,2*}, Masanobu Karasawa¹, Takahiro Asaka¹ and Masanori Owari^{1,3}

¹ Institute of Industrial Science, The University of Tokyo, 4-6-1 Komaba, Meguro-ku, Tokyo, 153-8505 Japan

² The Research Fellowship of Japan Society for the Promotion of Science

³ Environmental Science Center, The University of Tokyo, 7-3-1 Hongo, Bunkyo-ku, Tokyo, 113-0033 Japan

*m-mori@iis.u-tokyo.ac.jp

(Received : November 11, 2013; Accepted : January 31, 2014)

Atom probe tomography (APT) is a widely used technique to evaluate the atomic structure of semiconductor materials such as the field effect transistor. However, application of the APT technique faces difficulties, among which is the low reliability of reconstruction calculations due to poor understanding of the field evaporation mechanism. In general, lower detection efficiencies are observed in low evaporation field elements that undergo DC evaporation in APT. However, in the analysis of SiO₂ and GaAs, the detection efficiencies of oxygen and arsenic are higher than those of silicon and gallium, even though oxygen and arsenic have higher evaporation fields. To explain these phenomena, we evaluated the potential for neutral desorption from the sample surface without ionization in the APT analysis. We observed changes in the detection efficiencies of arsenic and phosphorus during analysis of InGaAsP, when the laser power and initial temperature were varied. This was attributed to increases in the temperature of the surface atoms during irradiation of the pulsed laser. Therefore, under the ultrahigh vacuum conditions applied in the experiment, the low vapor pressure elements might have experienced sublimation.

1. Introduction

Atom probe tomography (APT) is a unique three-dimensional imaging technique that is a powerful tool in materials science. Recently, the introduction of very short pulsed lasers into the atom probe instrument has allowed for the analysis of semiconductor materials such as electronic devices [1]. The two major advantages of APT, as compared to other microanalysis techniques, are its high spatial resolution and high detection sensitivity. In general, the atom probe instrument is a combination of a field ion microscope with a time-of-flight mass spectrometer and a delay line detector. The principle of this technique is based on field evaporation of surface atoms from a very sharp needle shaped sample of which the radius of curvature is less than 100 nm [2]. A high positive voltage potential is applied to the sample in order to generate a strong electrical field > 10 V/nm at the sample apex. The field-evaporated ions are accelerated and fly toward the delay line detector where the elemental identities of the evaporated ions are determined by time-of-flight mass spectrometry. The x-y position of each atom is calculated from the detected position and

the z position is calculated from the sequence of detection [3]. The 3D image of the micro region is created by this information at the atomic scale.

However, there are disadvantages with APT, including the susceptibility of sample rupture, the low reliability of reconstruction calculations, and the narrow analysis area [4]. Among these, the low reliability of the reconstruction calculation is very serious disadvantage, and is attributed to a poor understanding of the field evaporation mechanism. For example, an accurate reproduction of the electric field by the local electrode is very difficult to achieve. In addition, the sequence of field evaporation from a material containing elements of largely different evaporation fields is complex.

One of the most influential parameters to the reconstruction calculation is the detection efficiency, which was the focus of our study. In general, the detection efficiency of APT affects every element equally, and is limited by the aperture ratio of the microchannel plate and the effective detection area of field evaporation. However, different detection efficiencies on each element are often observed. This may be caused by elements in the

low evaporation field that evaporate without a trigger (pulsed laser) by DC high voltage, and thus cannot be detected with time-of-flight mass spectrometer. However, this explanation cannot be applied to every sample. For example, in the analysis of SiO₂ and GaAs, although oxygen and arsenic have a high evaporation field compared to silicon and gallium, the detection amount of oxygen or arsenic is lower than silicon or gallium, respectively. To explain this phenomenon, we evaluated the possibility of neutral desorption from the sample surface without ionization. When a pulsed laser was used as the trigger, the field evaporation mechanism was dependent on photon energy, thermal effects, and electric field modulation. In general, thermal effect is most dominant effect on evaporation [5]. When the pulsed laser irradiates, the temperatures of surface atoms increase drastically. Therefore, under ultrahigh vacuum conditions, the lower vapor pressure elements such as arsenic and phosphorus might undergo sublimation.

In this study, InGaAsP was analyzed by APT by varying the laser power and the initial temperature, and the detected amounts of arsenic and phosphorus were compared. To evaluate the detection efficiency dependent on laser irradiation, the spectrum was separated to the irradiation side and shadow side and compared. Moreover, the thermal distribution of the sample surface at laser irradiation was estimated by three methods.

2. Experiment

2.1. Dependence on sample temperature

In this study, InGaAsP (In : Ga : As : P = 1 : 10 : 8.5 : 2.5 in stoichiometry) was prepared for the analysis by APT. The evaporation fields of each element as reported in the literature are 12 V/nm (In⁺), 15 V/nm (Ga⁺) and 42 V/nm (As²⁺) [2], while phosphorus is unknown. The InGaAsP compound was formed by the focused ion beam (FIB, SMI3050, SIINT) micro sampling technique [2]. Finally, samples were cleaned of any residual pollution by field evaporation. Transmission electron microscopy (TEM, JEM-1010, JEOL, operated at 100 kV) was used to observe selected samples before and after the APT measurements. Samples were measured by a three-dimensional atom probe instrument developed in our laboratory [6]. The analyses were carried out using a pulsed laser with an initial sample temperature of 60 K or 300 K, pulse energy of 0.5-2.5 nJ/pulse, pulse repeti-

tion frequency of 5 kHz, wavelength of 532 nm, a laser spot size of approximately 20 μm and an evaporation rate of 5-10 ions per 100 pulses. The DC high voltage was changed to maintain a constant evaporation rate. To compare the number of detected atoms accurately, the detection volumes were the same.

To estimate the sample temperature under laser irradiation, the charge-state ratio method (CRM) was used. It has been reported that the ratio of W⁴⁺/(W³⁺+W⁴⁺) is changed by changing sample temperature under pulsed voltage evaporation [7]. Though CRM has not previously been applied to pulsed laser evaporation experiments, it was employed in the current study to qualitatively evaluate the temperature jump of the tip apex. Tungsten was formed for the APT sample by electropolishing in a 1M-NaOH solution, and this sample was cleaned by field evaporation. The sample was measured by APT with two wavelengths (1064 and 532 nm), and three or four levels of laser power, at an initial sample temperature of 60 K.

2.2. Estimation of temperature distribution between irradiation side and shadow side

To estimate the sample temperature distribution, three methods were employed: finite element method (FEM),

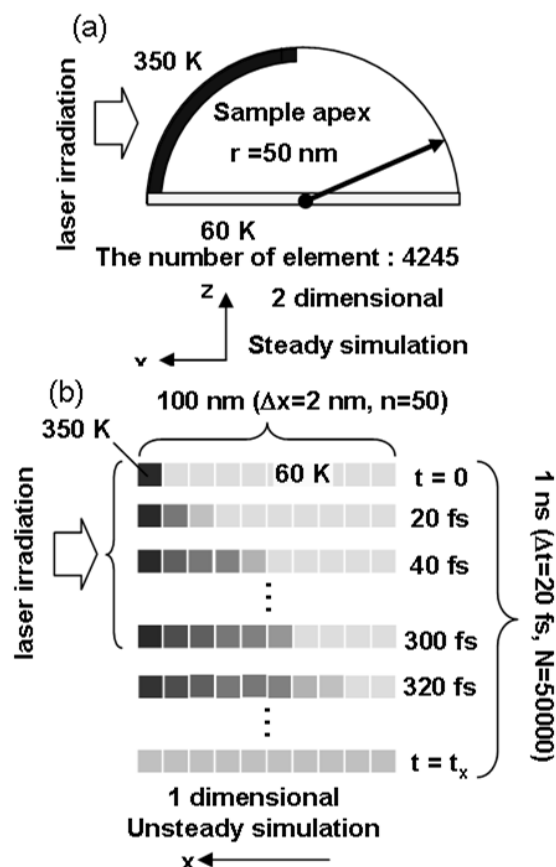


Fig. 1 The schematic of simulation conditions for (a) FEM and (b) FDM.

finite difference method (FDM), and charge-state ratio method (CRM). The FEM is a numerical technique for finding approximate solutions to boundary value problems for differential equations [8], while FDM is a numerical method for approximating the solutions to differential equations using finite difference equations to approximate derivatives [9].

The schematic images of FEM and FDM simulation conditions were compared (Fig. 1). For these methods, the temperature of the irradiation side surface at laser irradiation was set to 350 K[10]. For the CRM estimation, the tungsten sample was measured by APT with a laser power of 0.5-4.0 nJ/pulse. The mass spectra were separated to the irradiation side and shadow side, and the value of $W^{4+}/(W^{3+}+W^{4+})$ was calculated. The temperature of each side was estimated by CRM.

3. Results and Discussion

3.1. Dependence on sample temperature

The sample temperatures at varying levels of irradiation laser power were estimated by CRM (Fig. 2). The

sample temperatures at measured at both wavelengths were observed to increase depending on the laser power. The mass spectra of InGaAsP with an initial temperature of 60 K were measured during variations in the laser power (Fig. 3). The detection amount of arsenic and phosphorus are decreased depending on laser power. Although detection efficiencies have errors by mass resolution, its effect is slight. The mass spectra of InGaAsP were measured after varying the initial temperature (Fig. 4). At the same laser power, the detection amounts of arsenic and phosphorus were observed to change depending on initial temperature. The detection ratio between indium and gallium was not observed to change. However the ratio between arsenic and gallium appeared to change significantly (Figs. 3 and 4). These results indicated that the actual sample temperature (the sum of initial temperature and rise in temperature by laser irradiation) affected the detection efficiency of arsenic and phosphorus. Therefore, neutral evaporation from the sample surface might have occurred without ionization in APT.

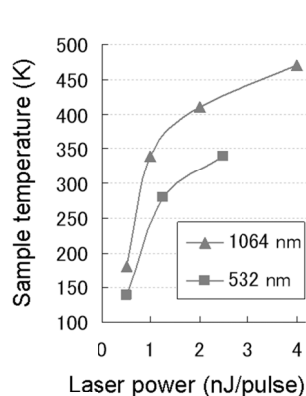


Fig. 2 Sample temperatures at each laser power estimated by CRM.

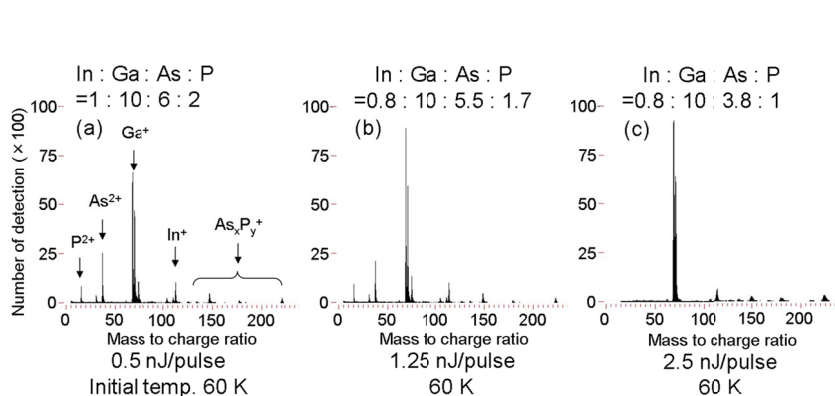


Fig. 3 Mass spectra of InGaAsP with initial temperature of 60 K measured by laser power of (a) 0.5, (B) 1.25 and (c) 2.5 nJ/pulse.

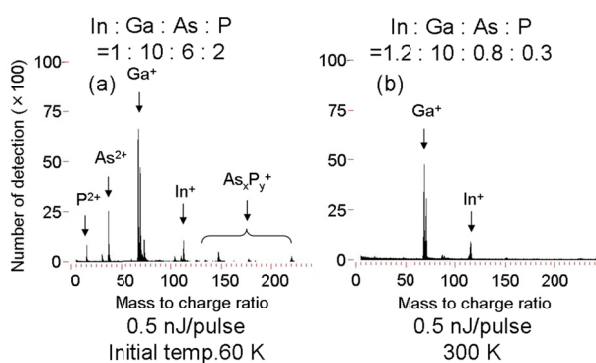


Fig. 4 Mass spectra of InGaAsP measured with initial temperature of (a) 60 and (b) 300 K.

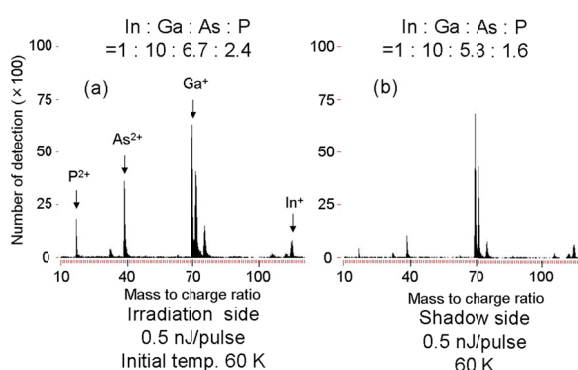


Fig. 5 Mass spectra of InGaAsP separated to (a) irradiation side and (b) shadow side.

3.2. Estimation of temperature distribution between irradiation side and shadow side

In the common APT setup, the laser irradiates the sample apex from a lateral direction. The opposite side of the sample to the laser beam remains in the shade (shadow side). The temperature on the sample surface is expected to increase due to the irradiation. In the study, the mass spectra of InGaAsP were separated between irradiation side and the shadow side and compared. The mass spectra of each side were measured with a laser power of 0.5 nJ/pulse and initial temperature of 60 K (Fig. 5). The detection efficiencies of arsenic and phosphorus were observed to be lower on the shadow side. This result did not agree with the previous experimental results that showed a dependence on temperature. To evaluate this result, the temperature distribution on the

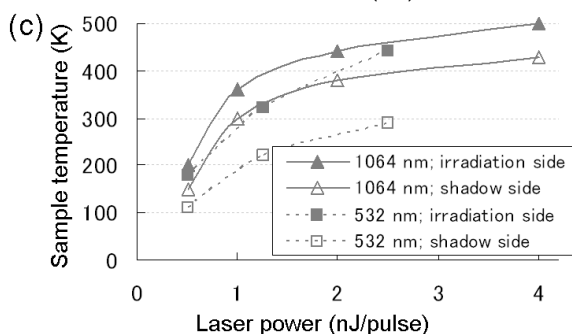
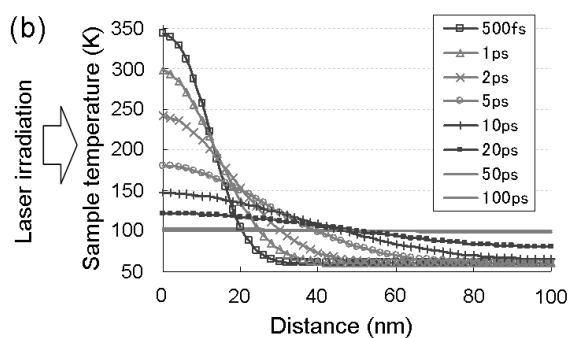
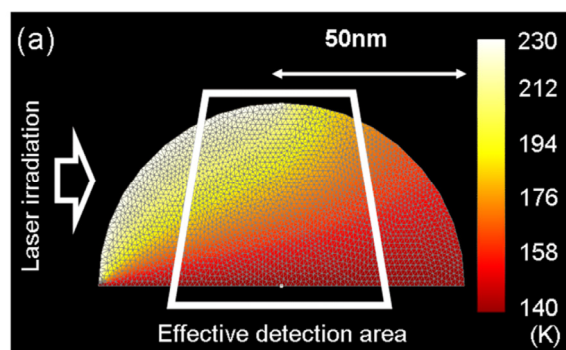


Fig. 6 Simulations of temperatures on sample surface. (a) FEM, (b) FDM and (c) CRM.

sample surface was simulated (Fig. 6). The difference of temperature between the irradiation side and the shadow side was estimated to be 100-200 K by FEM and FDM at a laser power of 0.5 nJ/pulse, while the difference was estimated to be 40-80 K by CRM. Although the laser irradiation conditions and sample geometry were not completely reproducible, the simulations indicated that a difference in degree of temperature rise occurred between the irradiation side and the shadow side. However, the detection efficiencies of arsenic and phosphorus were lower on the lower temperature shadow side. This was attributed to competition between the thermal energy and photon energy during field evaporation of arsenic and phosphorus. In our previous study, we reported that the ionization efficiency of an organic sample depends on the photon energy [11]. The lower detection efficiency observed on the shadow side in the current work was likely due to field evaporation that was influenced only by temperature, and that evaporation of neutral species also proceeded. Therefore, our results indicated that to achieve a high-precision APT analysis of an element that has a high vapor pressure and a high evaporation field, the sample temperature, DC high voltage, laser power, wavelength and pulse condition must be optimized according to materials. Shorter wavelengths in particular appeared to produce more accurate APT spectra due to the effects of higher photon energies and the inherent prevention of increasing sample temperatures.

4. Conclusion

The thermal distribution on a sample surface experiencing laser irradiation was estimated by three methods. The neutral evaporation from the sample surface might have occurred without ionization during APT. Our results indicated that achievement of a highly precise APT depends on optimization of the sample temperature, DC high voltage, laser power, wavelength, and pulse conditions according to materials.

5. Acknowledgement

This work was supported by Grant-in-Aid for Creative Scientific Research No. 18GS0204 and Research Fellowship from Japan Society for the Promotion of Science.

6. References

- [1] K. Inoue, F. Yano, A. Nishida, H. Takamizawa, T. Tsunomura, Y. Nagai, and M. Hasegawa, *Ultramicroscopy* **109**, 1479 (2009).
- [2] M. K. Miller, *Atom Probe Tomography: Analysis at Atomic Level*, Kluwer Academic, London (2000).
- [3] P. Bas, A. Bostel, B. Deconihout and D. Blavette, *Appl. Surf. Sci.* **87/88**, 298 (1995).
- [4] S. Kolling and W. Vandervorst, *Ultramicroscopy*, **109**, 486 (2009).
- [5] E. A. Marquis and B. Gault, *J. Appl. Phys.*, **104**, 084914 (2008).
- [6] N. Mayama, et al., *Surf. Interface Anal.*, **42**, 1616 (2010).
- [7] G. L. Kellogg, *J. Appl. Phys.*, **52**, 5320 (1981).
- [8] K. G. Ayappa, H. T. Davis, E. A. Davis and J. Gordon, *AIChE Journal*, **38**, 1577 (1992).
- [9] C. R. Chen, and H. S. Ramaswamy, *Chem. Eng. Process*, **46**, 603 (2007).
- [10] A. Cerezo, G. D. W. Smith and P. H. Clifton, *Appl. Phys. Lett.*, **88**, 154103 (2006).
- [11] Y. Kajiwara, Y. Hanaoka, N. Mayama, T. Iwata, M. Taniguchi, and M. Owari, *e-J. Surf. Sci. Nanotech.*, **8**, 217 (2010).